Eur. Phys. J. D **33**, 181–191 (2005)
DOI: 10.1140/epjd/e2005-00059-y

THE EUROPEAN PHYSICAL JOURNAL D

Radiative lifetime and oscillator strength determinations in Xe VI

É. Biémont[1,2,a], V. Buchard[2], H.-P. Garnir[1], P.-H. Lefèbvre[1], and P. Quinet[1,2]

[1] Institut de Physique Nucléaire, Atomique et de Spectroscopie, Université de Liège, Sart Tilman (Bât. B15), 4000 Liège, Belgium
[2] Astrophysique et Spectroscopie, Université de Mons-Hainaut, 7000 Mons, Belgium

Received 10 November 2004 / Received in final form 25 January 2005
Published online 3 May 2005 –

Abstract. Transition probabilities have been calculated for $\Delta n = 0$ and $\Delta n = 1$ transitions connecting the $5s^2nl$ [np ($n = 5$–8); nf ($n = 4$–5); nh ($n = 6$–8); nk ($n = 8$)], $5s5pnl$ ($nl = 5d$, $6s$), $5p^3$ and $5s^2nl$ [(ns ($n = 6$–8); nd ($n = 5$–8); ng ($n = 5$–6); ni ($n = 7$–8)] and $5s5p^2$ configurations of Xe VI. Core-polarization effects have been included in the framework of a Hartree-Fock approach. The accuracy of the present set of results has been assessed through comparisons with radiative lifetime measurements. Good agreement has been observed between theory and experiment.

PACS. 34.50.Fa Electronic excitation and ionization of atoms (including beam-foil excitation and ionization) – 32.30.Jc Visible and ultraviolet spectra

1 Introduction

The ground state of five-times ionized xenon (Xe VI), which belongs to the indium isoelectronic sequence, is $5s^25p\ ^2\mathrm{P}^o_{1/2}$. The spectrum of this ion is still poorly known not only regarding term analysis but also concerning line intensities and radiative parameter determinations while such data are needed in different fields of physics like astrophysics or plasma physics.

Only three transitions, at 59.984, 80.084 and 88.004 nm, were reported by Fawcett et al. [1] who analyzed high-temperature plasmas. Later on, a more detailed investigation of highly ionized xenon (Xe VI, Xe VII and Xe VIII) was due to Kernahan et al. [2] who analyzed beam-foil spectra between 50 and 155 nm at an energy of 1.6 MeV and were able to measure 4 lifetime values in Xe VI. Configuration interaction wavefunctions were used by Hibbert et al. [3] to predict energies and lifetimes of 22 levels of Xe VI. The results have been combined with experimental data to assign a number of previously unidentified lines and to correct other earlier assignments. Spectra of Xe, Cs, Ba and La (In isoelectronic sequence), produced with a high-voltage spark discharge, have been observed photographically by Kaufman and Sugar [4] and identified lines were used to determine the energy levels of the $5s^25p$, $5s5p^2$, $5s^25d$ and $5s^26s$ configurations. The $5s^25p\ ^2\mathrm{P}^o - 5s5p^2\ ^4\mathrm{P}$ intercombination transitions have been identified by Tauheed et al. [5] in indium-like ions from Sb III to La IX. Thirty-three lines (among them 5 of Xe VI) were classified, of which 20 were new.

Collision-based spectroscopy was the technique used by Larsson et al. [6] for investigating the spectra of Xe V and Xe VI. Eight Xe VI lines were classified, in particular transitions emitted from the $5s^24f$ configuration. The photon emission, from 60-keV Xe^{6+} ions colliding with Na and Ar, was recorded by Wang et al. [7,8] in the 35–800-nm wavelength range. Several of the observed lines were classified as transitions from singly excited states in Xe^{5+} and 11 new levels of Xe VI were established. In a second analysis [9], performed in the same wavelength domain, twenty-five new Xe VI lines were classified and twelve new levels were established, the analysis being supported by Hartree-Fock calculations.

In a recent work performed by Sarmiento et al. [10] the spectrum of Xe VI has been observed in the 27–700 nm range; 18 new levels in $5s5p6s$ configuration, all the energy levels in the $5p^3$ configuration and 3 levels in the $5s5p6s$ configuration have been deduced from this analysis using parametrized HFR calculations.

Transition probabilities or radiative lifetimes in Xe VI are still extremely fragmentary. The first effort for filling in this gap was due to Kernahan et al. [2] who were able to measure radiative lifetimes for 4 levels using the beam-foil spectroscopy technique. Ab initio transition probabilities have been calculated for 48 transitions of Xe VI and lifetime values reported for 17 levels by Hibbert et al. [3]. Weighted transition probabilities for a limited number (i.e. 25) of lines of the types $5s^2nl - 5s^2n'l'$ have been published by Wang et al. [9]. The most extensive work regarding the radiative parameters is due to Reyna Almandos et al. [11] who reported relativistic Hartree-Fock results for 104 spectral lines belonging to the $5s5p^2$, $5s^25d$, $5s^26s$ and $5s5p5d$, $5p^3$, $5s5p6s$ transition arrays in Xe VI. Calculated values of the lifetimes of the odd-configuration energy levels have been also presented by the same authors.

[a] e-mail: E.Biemont@ulg.ac.be

Transition probabilities have been calculated by Biémont et al. [12] in $5p^k$ configurations of Xe ions and along the corresponding isoelectronic sequences but they concern only forbidden transitions, while the present paper focuses on electric dipole transitions.

In view of this relative lack of transition probabilities in Xe VI, we present here a first detailed analysis of the intensity parameters of this ion. The results have been compared with radiative lifetime measurements performed with the beam-foil spectroscopy technique. An overall good agreement between theory and experiment has been observed.

2 Calculations

Calculations of energy levels and transition probabilities in Xe VI have been carried out using the Relativistic Hartree-Fock (HFR) approach [13] modified for taking core-polarization effects into account (see e.g. [14,15]). This method has been combined with a least-squares optimization process of the radial parameters in order to reduce as much as possible the discrepancies between Hamiltonian eigenvalues and experimental energy levels when available.

The following configurations were explicitly introduced in the calculations, the $5s^2nl$ Rydberg series being extended up to $n = 8$: $5s^25p+5s^26p+5s^27p+5s^28p+5s^24f+5s^25f+5s^26f+5s^27f+5s^28f+5s^26h+5s^27h+5s^28h+5s^28k+5s5p6s+5s5p5d+5s5p6d+5s5p5g+5s5p6g+5s5d4f+5s5d5f+5s6s4f+5s6s5f+5p^3+5p^26p+5p^24f+5p^25f$ and $5s^26s+5s^27s+5s^28s+5s^25d+5s^26d+5s^27d+5s^28d+5s^25g+5s^26g+5s^27g+5s^28g+5s^27i+5s^28i+5s5p^2+5s5d^2+5s6s^2+5s4f^2+5s5f^2+5s5p6p+5s5p4f+5s5p5f+5s5p6f+5p^26s+5p^25d+5p^26d$ for the two parities, respectively.

Core-polarization (CP) effects were introduced in the model in two different ways. In a first approach (calculation A), the $4s^24p^64d^{10}$ Pd-like core was considered for all the configurations by using the static dipole polarisability of Xe IX, i.e. $\alpha_d = 0.878$ a.u. according to the calculations of Fraga et al. [16] and by using a cut-off radius, provided by a HFR calculation and corresponding to the mean value $\langle r\rangle$ for the outer orbital of the configuration $4p^64d^{10}$, i.e. $r_c = 0.851$ a.u. In calculation B, the $4s^24p^64d^{10}5s^2$ Cd-like Xe VII core was considered for the transitions of the type $5s^2nl - 5s^2n'l'$ (excluding however transitions involving the $4f$ orbital which is strongly embedded in the core) with $\alpha_d = 4.520$ a.u., according to Johnson et al. [24] and $r_c = 1.690$, which corresponds to the HFR $\langle r\rangle$ value of the $5s^2$ orbital, the Pd-like core considered in calculation A being used for all other transition arrays.

In addition, the calculated eigenvalues of the Hamiltonian were adjusted to the observed energy levels as taken from Wang et al. [7–9] and Sarmiento et al. [10] in a least-squares fitting (LSF) procedure. More precisely, 46 odd levels belonging to the configurations $5s^25p$, $5s^26p$, $5s^27p$, $5s^28p$, $5s^24f$, $5s^25f$, $5s^26h$, $5s^27h$, $5s^28h$, $5s^28k$, $5p^3$, $5s5p5d$, $5s5p6s$ and 25 levels belonging to the configurations $5s^26s$, $5s^27s$, $5s^28s$, $5s^25d$, $5s^27d$, $5s^28d$, $5s^25g$, $5s^26g$, $5s^27i$, $5s^28i$, $5s5p^2$ were fitted.

For the configuration $5s^26d$, we were unable to reproduce the experimental level values established at 338400 cm^{-1} ($j = 3/2$) and 339770 cm^{-1}. This is mainly due to the fact that these two levels strongly interact with $5s5p4f$, this latter configuration extending from 273000 cm^{-1} to 343500 cm^{-1} according to our HFR calculations. Indeed, it was found that the $5s^26d$ composition varies from ∼75% to ∼20% when modifying the average energy of this configuration from ∼339000 cm^{-1} to ∼353000 cm^{-1}. Consequently, the numerical value of the E_{av} parameter corresponding to $5s^26d$ was fixed to 339574 cm^{-1} in order to have a coherent set of average energies along the Rydberg series.

For the one-configuration and configuration interaction Slater integrals, not modified in the LSF calculation, a scaling factor of 0.90 was applied. This scaling down of the F^k, G^k and R^k integrals is supposed to absorb the interactions with the myriad of distant configurations not considered explicitly in the model. The spin-orbit parameters, ζ_{nl}, not considered in the LSF procedure, were left at their ab initio values. This introduction of a scaling factor is justified on theoretical grounds [13] and the choice of the numerical value (i.e. 0.90) results from considerable experience of the authors of the present paper in calculations of atomic structure similar to those reported here.

The standard deviations of the fitting procedures for the even and odd levels were 345 and 423 cm^{-1}, respectively. The energy parameter values (in cm^{-1}) are reported in Table 1 for the $5s^2nl$ ($nl = 5-8p$, $4-5f$, $7-8h$, $8k$), $5s5p6s$, $5s5p5d$ and $5p^3$ configurations and in Table 2 for the $5s^2nl$ ($nl = 6-8s$, $5-8d$, $5-6g$, $7-8i$) and $5s5p^2$ configurations. A comparison between experimental and calculated energy level values is shown in Tables 3 and 4 where we report also the calculated percentage compositions (only the components of the eigenvectors larger than 5% are given).

3 Measurements

In order to assess the accuracy of the calculations, comparisons with experimental results have been performed. More precisely, lifetimes of 15 Xe VI levels have been measured by the beam-foil method [17], one of the rare methods able to produce this type of ions.

A beam of xenon ions was produced by a Van de Graaff accelerator of the University of Liège equipped with a conventional radio-frequency source. The beam was analyzed by a magnet and focused inside a target chamber. Beams of energies up to 2 MeV could be produced. Inside the chamber, the beam was excited and ionized by passing through a very thin (∼20 μg/cm^2) home-made carbon foil. Just after the foil, the light, emitted by the excited ions, was observed at right angle by a Seya-Namioka-type spectrometer equipped with a $R = 1$ m concave 1200 l/inch grating blazed for normal incidence at 110.0 nm. The entrance slit of the spectrometer had a width of 120 μm

Table 1. Adopted radial parameters for odd configurations. All the values are given in cm^{-1}.

Configuration	Parameter	Adopted value	Ratio
$5s^2 5p$	E_{av}	18754	-
	ζ_{5p}	10669	1.083
$5s^2 6p$	E_{av}	276994	-
	ζ_{6p}	3805	1.195
$5s^2 7p$	E_{av}	372637	-
	ζ_{7p}	1602	1.024
$5s^2 8p$	E_{av}	423805	-
	ζ_{8p}	905	1.018
$5s^2 4f$	E_{av}	193539	-
	ζ_{4f}	216	1.050
$5s^2 5f$	E_{av}	334553	-
	ζ_{5f}	73	1.037
$5s^2 6h$	E_{av}	428032	-
	ζ_{6h}	0.7	1.000f
$5s^2 7h$	E_{av}	457297	-
	ζ_{7h}	0.4	1.000f
$5s^2 8h$	E_{av}	476088	-
	ζ_{8h}	0.2	1.000f
$5s^2 8k$	E_{av}	476355	-
	ζ_{8k}	0.1	1.000f
$5s5p6s$	E_{av}	333940	-
	ζ_{5p}	9462	0.916
	$G^1(5s, 5p)$	68453	0.902
	$G^0(5s, 6s)$	4363	0.916
	$G^1(5p, 6s)$	6581	0.919
$5s5p5d$	E_{av}	284005	-
	ζ_{5p}	9352	0.933
	ζ_{5d}	742	1.023
	$F^2(5p, 5d)$	50142	1.074
	$G^1(5s, 5p)$	65983	0.877
	$G^2(5s, 5d)$	32615	0.913
	$G^1(5p, 5d)$	58507	1.077
	$G^3(5p, 5d)$	36875	1.066
$5p^3$	E_{av}	252882	-
	ζ_{5p}	9853	1.013
	$F^2(5p, 5p)$	50895	0.888
$5s^2 5p$–$5p^3$	$R^1(5s5s, 5p5p)$	71938	0.963
$5s^2 5p$–$5s5p5d$	$R^1(5s5p, 5p5d)$	52385	0.843
	$R^2(5s5p, 5p5d)$	38301	0.843
$5p^3$–$5s5p5d$	$R^1(5p5p, 5s5d)$	57186	0.926

f: fixed value. Ratio: fitted/HFR.

Table 2. Adopted radial parameters for even configurations. All the values are given in cm^{-1}.

Configuration	Parameter	Adopted value	Ratio
$5s^2 6s$	E_{av}	231942	-
$5s^2 7s$	E_{av}	352562	-
$5s^2 8s$	E_{av}	414162	-
$5s^2 5d$	E_{av}	184533	-
	ζ_{5d}	1026	1.454
$5s^2 6d$	E_{av}	339574	-
	ζ_{6d}	305	1.037
$5s^2 7d$	E_{av}	406949	-
	ζ_{7d}	160	1.017
$5s^2 8d$	E_{av}	442544	-
	ζ_{8d}	96	1.018
$5s^2 5g$	E_{av}	376930	-
	ζ_{5g}	1.6	1.000f
$5s^2 6g$	E_{av}	426325	-
	ζ_{6g}	0.9	1.000f
$5s^2 7i$	E_{av}	457264	-
	ζ_{7i}	0.3	1.000f
$5s^2 8i$	E_{av}	476193	-
	ζ_{8i}	0.2	1.000f
$5s5p^2$	E_{av}	131871	-
	ζ_{5p}	11011	1.125
	$F^2(5p, 5p)$	50855	0.888
	$G^1(5s, 5p)$	57017	0.764

f: fixed value. Ratio: fitted/HFR.

and was situated at 15 mm from the axis of the 10 mm diameter ion beam.

The light was detected by a thin, back-illuminated, liquid nitrogen cooled CCD detector specially developed for far UV measurements. The CCD detector system was supplied by the Universities of Leicester and Lund. It is based on a EEV CCD15-11 chip of 27.6×6.9 mm (1040×280 of 27×27 μm square pixels) specially conditioned for UV light detection [18,19]. The CCD works under vacuum and is cooled by liquid nitrogen to -90 °C for noise reduction. The CCD, which replaces the exit slit of the spectrometer, was tilted to an angle of 125° relatively to the spectrometer exit arm axis in order to be tangential to the Rowland circle. Under that geometry, it has a dispersion of 0.02 nm/pixel and detects light over a 20 nm wide region with a fairly constant resolution giving a line width (FWHM) of ∼0.12 nm. The whole system was working under vacuum (10^{-5} Torr). The CCD images were transferred to a networked computer and analyzed by a specially written software. The XY image was transformed by binning the horizontal lines into a file containing a list of numbers representing the light intensities as a function of the wavelength. The identification of Xe VI lines in our spectra was based on previously known levels [1–11].

A partial Grotrian diagram of Xe VI showing lines which have been measured at Liège is presented in Figure 1. Most of the lines were observed in second or third order where the efficiency of the spectrometer was higher [19]. For lifetime measurements, spectra have been recorded by moving the foil target upstream along the ion beam path. The measurements were made at beam energies of 1.9 MeV and 1.6 MeV. At these energies the charge state fraction of Xe VI is ∼20% and close to its maximum. The speed of the Xe ions after the foil has been calculated by taking the energy loss inside the foil into account [20]. For each spectrum and at each position, lines of interest have been fitted with Gaussian curves. The background has been subtracted and the amplitude of the Gaussian curve was recorded as a function of the distance after the foil.

The old beam-foil measurements were possibly affected by cascading problems due to non-selective excitation leading sometimes to too long lifetime values. Such effects are corrected in "modern" measurements by various

Table 3. Experimental and calculated energy level (in cm^{-1}) for odd configurations of Xe VI. Percentage compositions larger than 5% only are given.

E_{EXP}[a]	E_{HFR}	ΔE	Term	J	Composition
0	9	–9	$5s^25p\ ^2P^o$	1/2	97%
15599	15593	6	$5s^25p\ ^2P^o$	3/2	97%
184994	184699	295	$5s^24f\ ^2F^o$	5/2	97%
185306	185428	–122	$5s^24f\ ^2F^o$	7/2	96%
222992	223316	–324	$5p^3\ ^2D^o$	3/2	53% + 25% $5s5p(^3P)5d\ ^2D^o$ + 11% $5p^3\ ^2P^o$
227800	228011	–211	$5p^3\ ^2D^o$	5/2	66% + 33% $5s5p(^3P)5d\ ^2D^o$
232586	232445	141	$5p^3\ ^4S^o$	3/2	82% + 8% $5p^3\ ^2D^o$
245720	244983	737	$5s5p(^3P)5d\ ^4F^o$	3/2	96%
247209	247748	–539	$5s5p(^3P)5d\ ^4F^o$	5/2	96%
251646	251944	–298	$5s5p(^3P)5d\ ^4F^o$	7/2	96%
254634	254383	251	$5p^3\ ^2P^o$	1/2	75% + 17% $5s5p(^3P)5d\ ^2P^o$
258048	258320	–272	$5p^3\ ^2P^o$	3/2	54% + 19% $5s5p(^3P)5d\ ^2P^o$ + 9% $5p^3\ ^4S^o$
	258392		$5s5p(^3P)5d\ ^4F^o$	9/2	99%
	264472		$5s5p(^3P)5d\ ^4P^o$	5/2	64% + 27% $5s5p(^3P)5d\ ^4D^o$
264890	264896	–6	$5s^26p\ ^2P^o$	1/2	94%
265823	266045	–222	$5s5p(^3P)5d\ ^4D^o$	3/2	58% + 37% $5s5p(^3P)5d\ ^4P^o$
	266866		$5s5p(^3P)5d\ ^4D^o$	1/2	85% + 12% $5s5p(^3P)5d\ ^4P^o$
270303	270304	–1	$5s^26p\ ^2P^o$	3/2	93%
274528	274438	90	$5s5p(^3P)5d\ ^4P^o$	1/2	87% + 12% $5s5p(^3P)5d\ ^4D^o$
274659	274725	–66	$5s5p(^3P)5d\ ^4D^o$	5/2	69% + 21% $5s5p(^3P)5d\ ^4P^o$
274684	274315	369	$5s5p(^3P)5d\ ^4D^o$	7/2	95%
274826	274795	31	$5s5p(^3P)5d\ ^4P^o$	3/2	58% + 39% $5s5p(^3P)5d\ ^4D^o$
	277555		$5s5p(^3P)5d\ ^2F^o$	5/2	43% + 18% $5s5p(^1P)5d\ ^2F^o$ + 15% $5s5p(^3P)5d\ ^2D^o$
280522	279537	985	$5s5p(^3P)5d\ ^2D^o$	3/2	50% + 23% $5p^3\ ^2D^o$ + 17% $5s5p(^1P)5d\ ^2D^o$
281756	282752	–996	$5s5p(^3P)5d\ ^2D^o$	5/2	32% + 26% $5s5p(^3P)5d\ ^2F^o$ + 16% $5s5p(^1P)5d\ ^2D^o$
	290387		$5s5p(^3P)5d\ ^2F^o$	7/2	70% + 27% $5s5p(^1P)5d\ ^2F^o$
305944	305758	186	$5s5p(^3P)5d\ ^2P^o$	3/2	62% + 18% $5p^3\ ^2P^o$ + 13% $5s5p(^1P)5d\ ^2D^o$
309262	309300	–38	$5s5p(^3P)6s\ ^4P^o$	1/2	50% + 32% $5s5p(^3P)5d\ ^2P^o$ + 9% $5s5p(^3P)6s\ ^2P^o$
311133	310651	482	$5s5p(^3P)5d\ ^2P^o$	1/2	41% + 47% $5s5p(^3P)6s\ ^4P^o$ + 7% $5p^3\ ^2P^o$
313427	313648	–221	$5s5p(^3P)6s\ ^4P^o$	3/2	92%
314587	315051	–464	$5s5p(^1P)5d\ ^2F^o$	7/2	48% + 25% $5s^25f\ ^2F^o$ + 22% $5s5p(^3P)5d\ ^2F^o$
315931	316217	–286	$5s5p(^1P)5d\ ^2F^o$	5/2	45% + 30% $5s^25f\ ^2F^o$ + 19% $5s5p(^3P)5d\ ^2F^o$
	322048		$5s5p(^3P)6s\ ^2P^o$	1/2	84% + 7% $5s5p(^3P)5d\ ^2P^o$
323291	323047	244	$5s5p(^3P)6s\ ^4P^o$	5/2	99%
323779	323533	246	$5s5p(^1P)5d\ ^2D^o$	3/2	59% + 9% $5s5p(^1P)5d\ ^2P^o$ + 8% $5s5p(^3P)5d\ ^2P^o$
325434	325412	22	$5s5p(^1P)5d\ ^2D^o$	5/2	71% + 11% $5s5p(^3P)5d\ ^2D^o$ + 9% $5p^3\ ^2D^o$
326908	326247	661	$5s5p(^1P)5d\ ^2P^o$	1/2	84% + 6% $5p^3\ ^2P^o$
327651	327934	–283	$5s5p(^1P)5d\ ^2P^o$	3/2	68% + 9% $5s5p(^3P)6s\ ^2P^o$ + 6% $5p^3\ ^2P^o$
331652	331852	–200	$5s^25f\ ^2F^o$	7/2	71% + 21% $5s5p(^1P)5d\ ^2F^o$
331929	332243	–314	$5s^25f\ ^2F^o$	5/2	65% + 24% $5s5p(^1P)5d\ ^2F^o$ + 6% $5s5p(^3P)5d\ ^2F^o$
	332459		$5s5p(^3P)6s\ ^2P^o$	3/2	79% + 12% $5s5p(^1P)5d\ ^2P^o$
	363765		$5s5p(^1P)6s\ ^2P^o$	1/2	66% + 31% $5s^27p\ ^2P^o$
	365236		$5s5p(^1P)6s\ ^2P^o$	3/2	74% + 21% $5s^27p\ ^2P^o$
374180	374618	–438	$5s^27p\ ^2P^o$	1/2	68% + 29% $5s5p(^1P)6s\ ^2P^o$
375500	376075	–575	$5s^27p\ ^2P^o$	3/2	78% + 21% $5s5p(^1P)6s\ ^2P^o$
423270	423074	196	$5s^28p\ ^2P^o$	1/2	99%
424230	424399	–169	$5s^28p\ ^2P^o$	3/2	98%
427561	427574	–13	$5s^26h\ ^2H^o$	9/2	94%
427561	427548	13	$5s^26h\ ^2H^o$	11/2	99%
456857	456851	6	$5s^27h\ ^2H^o$	9/2	99%
456857	456863	–6	$5s^27h\ ^2H^o$	11/2	99%
475837	475816	21	$5s^28h\ ^2H^o$	9/2	96%
475837	475858	–21	$5s^28h\ ^2H^o$	11/2	96%
476355	476355	0	$5s^28k\ ^2K^o$	13/2	100%
476355	476355	0	$5s^28k\ ^2K^o$	15/2	100%

[a] From Wang et al. [7–9] and Sarmiento et al. [10].

Table 4. Experimental and calculated energy level (in cm^{-1}) for even configurations of Xe VI. Percentage compositions larger than 5% only are given.

E_{EXP} [a]	E_{HFR}	ΔE	Term	J	Composition
92586	92824	–238	$5s5p^2\ ^4$P	1/2	94%
100378	100855	–477	$5s5p^2\ ^4$P	3/2	98%
107205	107462	–257	$5s5p^2\ ^4$P	5/2	85% + 14% $5s5p^2\ ^2$D
124870	123638	1232	$5s5p^2\ ^2$D	3/2	83% + 11% $5s^25d\ ^2$D
129230	128073	1157	$5s5p^2\ ^2$D	5/2	74% + 14% $5s5p^2\ ^4$P + 10% $5s^25d\ ^2$D
141837	141837	0	$5s5p^2\ ^2$P	1/2	66% + 28% $5s5p^2\ ^2$S
157996	159036	–1040	$5s5p^2\ ^2$S	1/2	65% + 31% $5s5p^2\ ^2$P
159112	159198	–86	$5s5p^2\ ^2$P	3/2	92%
180250	180413	–164	$5s^25d\ ^2$D	3/2	83% + 12% $5s5p^2\ ^2$D
182308	182449	–141	$5s^25d\ ^2$D	5/2	85% + 10% $5s5p^2\ ^2$D
223478	223475	3	$5s^26s\ ^2$S	1/2	97%
338450			$5s^26d\ ^2$D	3/2	
339770			$5s^26d\ ^2$D	5/2	
352250	352256	–6	$5s^27s\ ^2$S	1/2	99%
376933	376931	2	$5s^25g\ ^2$G	7/2	96%
376933	376935	–2	$5s^25g\ ^2$G	9/2	96%
404100	403885	215	$5s^27d\ ^2$D	3/2	77% + 21% $5s5p(^1$P$)6p\ ^2$D
404930	405135	–205	$5s^27d\ ^2$D	5/2	84% + 14% $5s5p(^1$P$)6p\ ^2$D
413710	413596	114	$5s^28s\ ^2$S	1/2	52% + 36% $5s5p(^1$P$)6p\ ^2$P + 7% $5s5p(^1$P$)6p\ ^2$S
426186	426075	111	$5s^26g\ ^2$G	7/2	96%
426186	426308	–122	$5s^26g\ ^2$G	9/2	87%
442770	442783	–13	$5s^28d\ ^2$D	3/2	96%
443150	443145	5	$5s^28d\ ^2$D	5/2	78% + 8% $5p^2(^1$S$)5d\ ^2$D + 6% $5p^2(^3$P$)5d\ ^2$D
457264	457263	1	$5s^27i\ ^2$I	11/2	100%
457264	457265	–1	$5s^27i\ ^2$I	13/2	100%
476192	476191	1	$5s^28i\ ^2$I	11/2	100%
476192	476193	–1	$5s^28i\ ^2$I	13/2	100%

[a] From Wang et al. [7–9] and Sarmiento et al. [10].

procedures like the so-called arbitrarily-normalized decay-curve (ANDC) technique, a method originally suggested by Curtis et al. [21]. In Xe V for example, the experimental beam-foil results of Pinnington et al. [23] were mean results deduced using both the multi-exponential curve fitting routines HOMER and TROY on the one hand and a routine including the data close to the foil corrected for the vignetting induced by the foil holder on the other hand. However, in view of the complexity of the energy levels scheme and of the lack of information about the eventual cascades, these procedures are sometimes applied with difficulty and special care has to be exercised [22].

In the present work, the experimental data have been fitted with a model describing the whole decay curve as a growing part (close to the foil) followed by a multi-exponential decay to take into account the possible cascading process. The lifetime of the upper level of the transition has been deduced from the value of the decay constant of the main exponential contribution. A sample of decay curve, as observed in the present work, is illustrated in Figure 2. The theoretical and experimental lifetimes values obtained in this study are reported and compared in Table 5. For a better understanding of the accuracy and limitations of the results reported in the table, the following comments about the different levels are relevant.

3.1 $5s^26s\ ^2S_{1/2}$

A lifetime of 0.050 ± 0.005 ns has been obtained from the analysis of the 44.75 nm line observed in the third order (Fig. 2). The primary component was embedded in a strong secondary component having a lifetime of ∼0.9 ns. There is no clear explanation for this secondary component. The other component of the multiplet (at 48.10 nm) was observed but it was not possible to obtain a reliable lifetime from its analysis.

3.2 $5s^26p\ ^2P^o_{1/2}$

The lifetime of this level (0.20 ± 0.02 ns), obtained from the 71.42 nm line, is substantially larger than the value reported previously by [2] but is in agreement with the theoretical prediction. The transition at 71.42 nm is blended with the line at 71.43 nm. The lifetime of the upper level of the transition at 71.43 nm has been measured through another depopulating channel at 79.76 nm and found also in agreement with the HFR result. It is therefore expected that the contribution of the 71.43 nm transition to the blend is small due to the fact that the log gf is −0.35 (compared to 0.05 for the line at 79.76 nm).

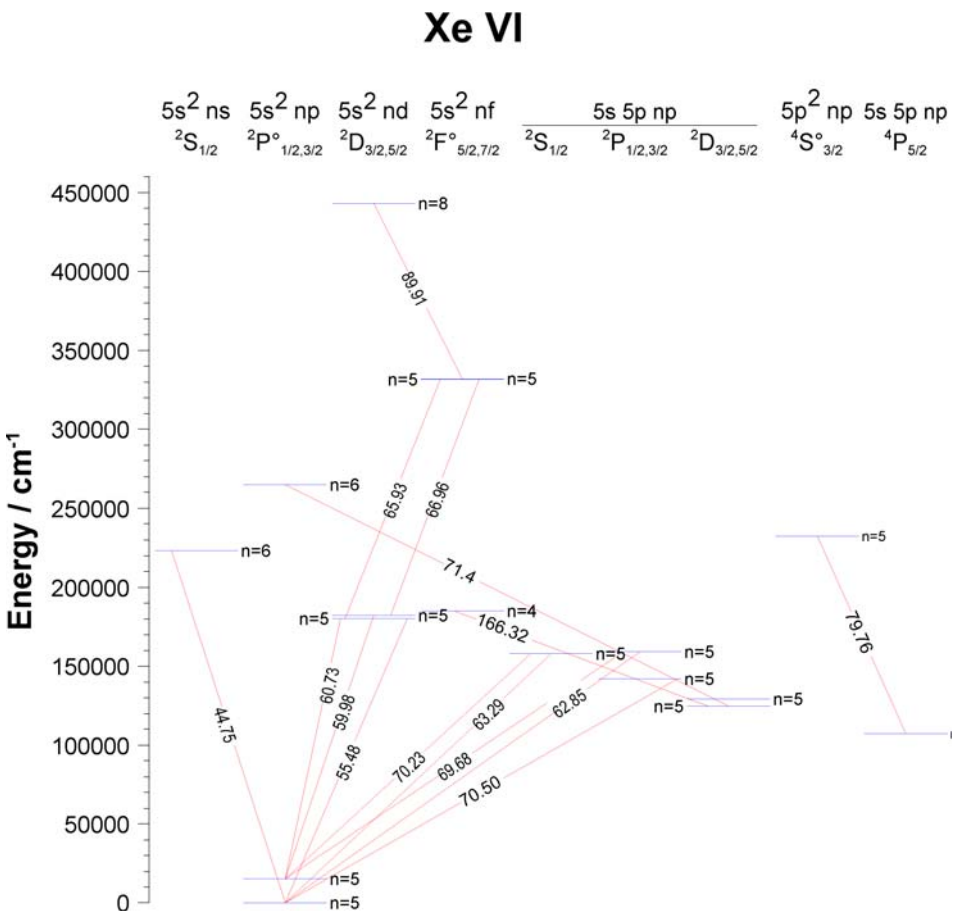

Fig. 1. Partial Grotrian diagram of Xe VI showing lines (wavelengths in nm) which lifetimes have been measured.

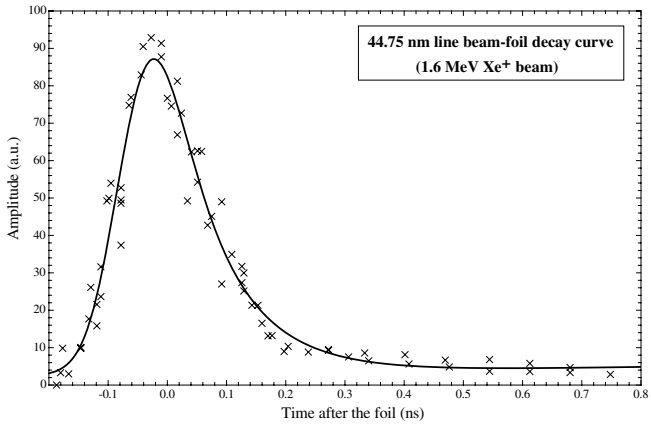

Fig. 2. Beam-foil decay curve of the 44.75 nm transition of XeVI. The black line results from a fit of a sum of two decaying exponentials (0.05 and 0.1 ns) plus a background convoluted with a Gaussian shaped instrumental response.

3.3 $5s^2 5d\ ^2D_{3/2,5/2}$

The mean lifetime of the term is 0.12 ns and has been evaluated from three lines of the $5p^2P^o - 5d^2D$ multiplet observed in the second order (see Tab. 5). The experimental values are in good agreement with the calculations for $J = 3/2$. For $J = 5/2$, the theoretical lifetime appears somewhat larger than the experiment. The present experimental result however is in close agreement with the measurement of Kernahan et al. [2] obtained with the same experimental technique.

3.4 $5s^2 8d\ ^2D_{5/2}$

This level is the only one for which the HFR result disagrees substantially from the beam-foil measurement. A possible explanation for this discrepancy is the fact that configuration interactions with higher members along the Rydberg series are not taken into account in our theoretical model (the series being limited to $n = 8$). Further measurements and/or calculations would be necessary to definitely settle the question.

3.5 $5s^2 4f\ ^2F^o_{5/2}$

This level lifetime has been obtained by analyzing the strong 166.3 nm line observed in the first order of the grating. Due to the lack of theoretical prediction for that level, the proposed value (0.096 ns) could not be compared with theory.

Table 5. Experimental and theoretical lifetime values (in ns) in Xe VI.

Xe VI lines			Experiment		Theory	
λ (nm)	Order	Transition	This work	Previous	This work	Previous
44.75	3	$5s^25p\ ^2P^\circ_{1/2} - 5s^26s\ ^2S_{1/2}$	0.050 ± 0.005		0.05	0.0079[c]
55.48	3	$5s^25p\ ^2P^\circ_{1/2} - 5s^25d\ ^2D_{3/2}$	0.10 ± 0.02	0.11[a]	0.13	0.046[c]
59.98	2	$5s^25p\ ^2P^\circ_{3/2} - 5s^25d\ ^2D_{5/2}$	0.12 ± 0.02	0.12[a]	0.17	0.052[c]
60.73	2	$5s^25p\ ^2P^\circ_{3/2} - 5s^25d\ ^2D_{3/2}$	0.13 ± 0.02		0.13	0.046[c]
62.85	2bl	$5s^25p\ ^2P^\circ_{1/2} - 5s5p^2\ ^2P_{3/2}$	0.10 ± 0.01		0.09	0.060[c]
63.29	2w	$5s^25p\ ^2P^\circ_{1/2} - 5s5p^2\ ^2S_{1/2}$	0.12 ± 0.03		0.15	0.12[c]
65.93	2	$5s^25d\ ^2D_{3/2} - 5s^25f\ ^2F^\circ_{5/2}$	0.05 ± 0.02		0.05	
66.96	2	$5s^25d\ ^2D_{5/2} - 5s^25f\ ^2F^\circ_{7/2}$	0.06 ± 0.02		0.06	
69.68	2	$5s^25p\ ^2P^\circ_{3/2} - 5s5p^2\ ^2P_{3/2}$	0.11 ± 0.02		0.09	0.060[c]
70.23	2	$5s^25p\ ^2P^\circ_{3/2} - 5s5p^2\ ^2S_{1/2}$	0.18 ± 0.02		0.15	0.12[c]
70.50	2	$5s^25p\ ^2P^\circ_{1/2} - 5s5p^2\ ^2P_{1/2}$	0.14 ± 0.02		0.12	0.079[c]
71.42	2	$5s5p^2\ ^2D_{3/2} - 5s^2\ 6p\ ^2P^\circ_{1/2}$	0.20 ± 0.02		0.24	0.144[c]
79.76	2	$5s5p^2\ ^4P_{5/2} - 5p^3\ ^4S^\circ_{3/2}$	0.12 ± 0.02		0.14	0.075[c]
89.91	2	$5s^25f\ ^2F^\circ_{5/2} - 5s^28d\ ^2D_{5/2}$	0.10 ± 0.02		0.17	
166.30	1	$5s5p^2\ ^2D_{3/2} - 5s^24f\ ^2F^\circ_{5/2}$	0.096 ± 0.020		-	0.47[c]

[a] Kernahan et al. [2]. [b] Reyna Almandos et al. [11]. [c] Hibbert et al. [3]. bl: Blend; w: weak.

3.6 $5s^25f\ ^2F^o_{5/2,7/2}$

Two lines of the $5d\ ^2D - 5f\ ^2F^o$ multiplet, at 65.93 and 66.96 nm, respectively, have been analyzed. The lifetimes deduced from the $5/2 - 7/2$ transition ($\tau = 0.06$ ns) and from the $3/2 - 5/2$ component ($\tau = 0.05$ ns) are close to the theoretical estimates. Note that the difference in lifetimes between the $5f$ and, e.g. the $5d$ configuration, as predicted by theory, is well reproduced by the experiment.

3.7 $5s5p^2\ ^2S_{1/2}$

Two lines originating from this level have been analyzed. The line at 63.29 nm was weak, its decay analysis was difficult and led to a value (0.12 ± 0.03 ns). Another experimental lifetime (0.18 ± 0.02 ns) was deduced from the analysis of the 70.23 nm line observed in the second order. The average of the two experimental results confirms the theoretical prediction (0.15 ns).

3.8 $5s5p^2\ ^2P_{1/2,3/2}$

Two lines originating from the $J = 3/2$ level have been measured. The lifetime deduced from the analysis of the line at 62.85 nm is 0.10 ± 0.01 ns. This transition, in our spectra, is partly blended with a weak line at 62.94 nm and, for each wavelength, a fitting profile describing the two components has been used. However, as the 62.94 nm line has a shorter lifetime of ∼0.009 ns, its influence on the decay analysis of the 62.85 ns line is not essential. The other line originating from the $J = 3/2$ level (69.68 nm) gives a lifetime of 0.11 ± 0.02 ns in close agreement with the above value. The lifetime of the $J = 1/2$ level (0.14 ± 0.02 ns) has been obtained by analyzing a line at 70.50 nm. These two levels ($J = 1/2$ and $3/2$) have both experimentally and theoretically determined lifetime values in approximatively the same ratio (∼1.3). For $J = 1/2$, our lifetimes are considerably larger than the results reported by [2] but the HFR results give strong support to our measurements.

3.9 $5p^3\ ^4S^o_{3/2}$

The experimental value (0.12 ± 0.02 ns) has been obtained from the observation of the 79.76 nm line. For this level, theory and experiment agree reasonably well (within 17%).

4 Conclusions

Transition probabilities have been calculated for $\Delta n = 0$ and $\Delta n = 1$ transitions of Xe VI. Core-polarization effects have been included in the framework of a Hartree-Fock approach. For most of the levels, a good agreement is observed between calculated and experimental lifetime values measured by beam-foil spectroscopy. This agreement gives more weight to the physical model adopted for the calculations.

The weighted oscillator strengths ($\log gf$) for the transitions connecting the $5s^2nl$ [np ($n = 5$–8); nf ($n = 4$–5); nh ($n = 6$–8); nk ($n = 8$), $5s5pnl$ ($nl = 5d, 6s$), $5p^3$ and $5s^2nl$ [($ns = 6$–8); nd ($nd = 5$–8); ng ($ng = 5$–6); ni ($ni = 7$–8)] and $5s5p^2$ configurations are reported in Table 6. In view of the space limitations, only the strongest transitions ($\log gf > -1.0$) are given in the table.

A limitation to the accuracy of the results reported in Table 6 might possibly originate from cancellation effects affecting the line strengths. In fact, this is not the case because, for all the transitions quoted in Table 6, it has

Table 6. Calculated oscillator strengths for transitions in Xe VI. Only log gf greater than –1 are reported in the table. Air wavelengths and vacuum wavelengths are given above and below 200.0 nm, respectively.

λ (nm)	Lower level			Upper level			log gf
	E (cm^{-1})	J	Parity*	E (cm^{-1})	J	Parity*	
29.7044	15599	3/2	o	352250	1/2	e	–0.87
44.7472	0	1/2	o	223478	1/2	e	–0.40
44.8606	100378	3/2	e	323291	5/2	o	–0.22
45.2814	92586	1/2	e	313427	3/2	o	–0.23
46.2133	159112	3/2	e	375500	3/2	o	–0.88
46.2568	157996	1/2	e	374180	1/2	o	–0.98
46.2779	107205	5/2	e	323291	5/2	o	0.07
46.9376	100378	3/2	e	313427	3/2	o	–0.85
47.4485	100378	3/2	e	311133	1/2	o	–0.59
47.8735	100378	3/2	e	309262	1/2	o	–0.60
48.1050	15599	3/2	o	223478	1/2	e	–0.13
48.2202	107205	5/2	e	314587	7/2	o	–0.40
48.2954	124870	3/2	e	331929	5/2	o	–0.83
48.4914	107205	5/2	e	313427	3/2	o	–0.21
49.3143	124870	3/2	e	327651	3/2	o	–0.86
50.3979	129230	5/2	e	327651	3/2	o	–0.70
51.4009	129230	5/2	e	323779	3/2	o	–0.87
51.5302	129230	5/2	e	323291	5/2	o	–0.76
51.5649	180250	3/2	e	374180	1/2	o	–0.66
51.7620	182308	5/2	e	375500	3/2	o	–0.51
52.3393	124870	3/2	e	315931	5/2	o	0.49
53.5615	129230	5/2	e	315931	5/2	o	–0.77
53.9499	129230	5/2	e	314587	7/2	o	0.59
54.0334	141837	1/2	e	326908	1/2	o	0.08
54.2323	124870	3/2	e	309262	1/2	o	–0.96
54.9626	141837	1/2	e	323779	3/2	o	0.10
55.4786	0	1/2	o	180250	3/2	e	0.42
57.2935	251646	7/2	o	426186	9/2	e	–0.38
57.3237	100378	3/2	e	274826	3/2	o	0.22
57.3786	100378	3/2	e	274659	5/2	o	0.12
57.4218	100378	3/2	e	274528	1/2	o	0.07
57.7244	92586	1/2	e	265823	3/2	o	0.35
57.8546	270303	3/2	o	443150	5/2	e	–0.84
59.3334	159112	3/2	e	327651	3/2	o	0.25
59.5962	159112	3/2	e	326908	1/2	o	–0.22
59.6584	107205	5/2	e	274826	3/2	o	–0.05
59.7090	107205	5/2	e	274684	7/2	o	0.78
59.7179	107205	5/2	e	274659	5/2	o	0.50
59.9848	15599	3/2	o	182308	5/2	e	0.68
60.1243	159112	3/2	e	325434	5/2	o	0.84
60.3197	157996	1/2	e	323779	3/2	o	0.33
60.4368	92586	1/2	e	258048	3/2	o	–0.96
60.4430	100378	3/2	e	265823	3/2	o	–0.30
60.7286	159112	3/2	e	323779	3/2	o	–0.37
60.7347	15599	3/2	o	180250	3/2	e	–0.08
60.9359	141837	1/2	e	305944	3/2	o	0.46
62.8488	0	1/2	o	159112	3/2	e	–0.16
63.7405	124870	3/2	e	281756	5/2	o	–0.98
64.2458	124870	3/2	e	280522	3/2	o	0.37
65.3008	157996	1/2	e	311133	1/2	o	–0.09
65.5625	129230	5/2	e	281756	5/2	o	0.48
65.7799	223478	1/2	e	375500	3/2	o	–0.39
65.9285	180250	3/2	e	331929	5/2	o	0.85
66.0057	274684	7/2	o	426186	9/2	e	–0.83
66.0973	129230	5/2	e	280522	3/2	o	–0.78

* e: even; o: odd.

Table 6. *Continued.*

λ (nm)	Lower level			Upper level			log gf
	E (cm^{-1})	J	Parity*	E (cm^{-1})	J	Parity*	
66.1085	157996	1/2	e	309262	1/2	o	–0.20
66.3560	223478	1/2	e	374180	1/2	o	–0.51
66.7605	124870	3/2	e	274659	5/2	o	–0.92
66.8355	182308	5/2	e	331929	5/2	o	–0.13
66.9595	182308	5/2	e	331652	7/2	o	0.99
67.1953	264890	1/2	o	413710	1/2	e	–0.09
67.5911	157996	1/2	e	305944	3/2	o	–0.45
67.8420	180250	3/2	e	327651	3/2	o	–0.11
68.1050	159112	3/2	e	305944	3/2	o	–0.08
68.1857	180250	3/2	e	326908	1/2	o	–0.01
68.6832	129230	5/2	e	274826	3/2	o	–0.93
68.7502	129230	5/2	e	274684	7/2	o	–0.25
68.8028	182308	5/2	e	327651	3/2	o	–0.08
69.2324	107205	5/2	e	251646	7/2	o	–0.72
69.6721	180250	3/2	e	323779	3/2	o	0.04
69.6801	15599	3/2	o	159112	3/2	e	0.38
69.8685	182308	5/2	e	325434	5/2	o	0.31
70.2264	15599	3/2	o	157996	1/2	e	–0.05
70.5034	0	1/2	o	141837	1/2	e	0.08
70.6859	182308	5/2	e	323779	3/2	o	–0.39
70.8852	129230	5/2	e	270303	3/2	o	–0.31
71.4183	124870	3/2	e	264890	1/2	o	–0.56
71.4286	92586	1/2	e	232586	3/2	o	–0.35
71.8339	264890	1/2	o	404100	3/2	e	–0.82
72.1060	141837	1/2	e	280522	3/2	o	–0.46
72.8831	305944	3/2	o	443150	5/2	e	–0.73
73.7021	180250	3/2	e	315931	5/2	o	–0.21
74.2793	270303	3/2	o	404930	5/2	e	–0.98
75.5978	182308	5/2	e	314587	7/2	o	0.04
75.6384	100378	3/2	e	232586	3/2	o	–0.05
77.0629	124870	3/2	e	254634	1/2	o	–0.37
77.6288	129230	5/2	e	258048	3/2	o	–0.19
79.7569	107205	5/2	e	232586	3/2	o	0.05
80.0834	0	1/2	o	124870	3/2	e	–0.50
80.8826	182308	5/2	e	305944	3/2	o	–0.99
81.5368	159112	3/2	e	281756	5/2	o	–0.78
82.3655	159112	3/2	e	280522	3/2	o	–0.93
83.7724	323779	3/2	o	443150	5/2	e	–0.91
86.3655	107205	5/2	e	222992	3/2	o	–0.63
88.0043	15599	3/2	o	129230	5/2	e	–0.62
101.0754	159112	3/2	e	258048	3/2	o	–0.71
101.1081	376933	7/2	e	475837	9/2	o	–0.59
101.1081	376933	9/2	e	475837	11/2	o	–0.45
101.4506	129230	5/2	e	227800	5/2	o	–0.48
101.9138	124870	3/2	e	222992	3/2	o	–0.85
103.4785	157996	1/2	e	254634	1/2	o	–0.89
105.7820	331652	7/2	o	426186	9/2	e	–0.62
106.0929	331929	5/2	o	426186	7/2	e	–0.56
110.6893	314587	7/2	o	404930	5/2	e	–0.89
111.0452	180250	3/2	e	270303	3/2	o	–0.91
111.1964	323779	3/2	o	413710	1/2	e	–0.78
113.4185	315931	5/2	o	404100	3/2	e	–0.81
113.6428	182308	5/2	e	270303	3/2	o	0.06
114.4689	264890	1/2	o	352250	1/2	e	–0.25
115.2047	326908	1/2	o	413710	1/2	e	–0.82

* e: even; o: odd.

Table 6. *Continued.*

λ (nm)	Lower level			Upper level			log gf
	E (cm^{-1})	J	Parity*	E (cm^{-1})	J	Parity*	
118.1469	180250	3/2	e	264890	1/2	o	–0.21
122.0301	270303	3/2	o	352250	1/2	e	0.01
123.2213	141837	1/2	e	222992	3/2	o	–0.92
125.1189	376933	7/2	e	456857	9/2	o	0.07
125.1189	376933	9/2	e	456857	11/2	o	0.16
136.4666	331652	7/2	o	404930	5/2	e	–0.51
138.5598	331929	5/2	o	404100	3/2	e	–0.50
145.5858	159112	3/2	e	227800	5/2	o	–0.80
147.8197	375500	3/2	o	443150	5/2	e	–0.82
160.3952	314587	7/2	o	376933	9/2	e	0.31
163.9291	315931	5/2	o	376933	7/2	e	0.26
194.1785	325434	5/2	o	376933	7/2	e	–0.79
197.5192	376933	7/2	e	427561	9/2	o	1.05
197.5192	376933	9/2	e	427561	9/2	o	–0.60
197.5192	376933	9/2	e	427561	11/2	o	1.16
201.3408	426186	7/2	e	475837	9/2	o	0.29
201.3408	426186	9/2	e	475837	11/2	o	0.40
205.5643	427561	9/2	o	476192	11/2	e	0.34
213.4929	223478	1/2	e	270303	3/2	o	0.17
220.7743	331652	7/2	o	376933	7/2	e	–0.80
220.7743	331652	7/2	o	376933	9/2	e	0.74
222.1333	331929	5/2	o	376933	7/2	e	0.59
241.4013	223478	1/2	e	264890	1/2	o	–0.17
252.8964	374180	1/2	o	413710	1/2	e	–0.73
261.6335	375500	3/2	o	413710	1/2	e	0.04
325.9469	426186	7/2	e	456857	9/2	o	1.03
325.9469	426186	9/2	e	456857	9/2	o	–0.66
325.9469	426186	9/2	e	456857	11/2	o	1.08
334.1285	374180	1/2	o	404100	3/2	e	0.14
336.5696	427561	9/2	o	457264	11/2	e	1.26
336.5696	427561	11/2	o	457264	11/2	e	–0.53
336.5696	427561	11/2	o	457264	13/2	e	1.36
339.6918	375500	3/2	o	404930	5/2	e	0.53
349.5503	375500	3/2	o	404100	3/2	e	–0.53
429.9866	352250	1/2	e	375500	3/2	o	0.29
455.8686	352250	1/2	e	374180	1/2	o	–0.10
496.6324	404100	3/2	e	424230	3/2	o	–0.58
512.6776	423270	1/2	o	442770	3/2	e	0.62
517.0528	456857	9/2	o	476192	11/2	e	1.23
517.0528	456857	11/2	o	476192	11/2	e	–0.59
517.9904	404930	5/2	e	424230	3/2	o	0.40
521.5032	404100	3/2	e	423270	1/2	o	0.10
523.6612	457264	11/2	e	476355	13/2	o	1.45
523.6612	457264	13/2	e	476355	13/2	o	–0.51
523.6612	457264	13/2	e	476355	15/2	o	1.51
528.3942	424230	3/2	o	443150	5/2	e	0.75
538.2663	457264	13/2	e	475837	11/2	o	–0.94
539.2244	424230	3/2	o	442770	3/2	e	–0.12
950.3096	413710	1/2	e	424230	3/2	o	0.12

* e: even; o: odd.

been verified that the cancellation factor, as defined in reference [13], is larger than 0.01 indicating that such effects are not present.

For the different reasons outlined above, we are confident in the accuracy of the gf values reported in Table 6 which constitute probably the most accurate set of results presently available in this ion.

Financial support from the Belgian Institut Interuniversitaire des Sciences Nucléaires (IISN) and from the FNRS is acknowledged. Two of us (E.B. and P.Q.) are respectively Research Director and Research Associate of this organism. The cooperation of the accelerator staff (M. Clar and A. Dresse) during the acquisition of data is gratefuly acknowledged. The authors are grateful to the anonymous referees for a careful reading of the manuscript.

References

1. B.C. Fawcett, B.B. Jones, R. Wilson, Proc. Phys. Soc. A **78**, 1223 (1961)
2. J.A. Kernahan, E.H. Pinnington, J.A. O'Neill, J.L. Bahr, K.E. Donelly, J. Opt. Soc. Am. **70**, 1126 (1980)
3. A. Hibbert, J.A. Kernahan, E.H. Pinnington, F.R. Simpson, Nucl. Instrum. Meth. **202**, 329 (1982)
4. V. Kaufman, J. Sugar, J. Opt. Soc. Am. B **4**, 1924 (1987)
5. A. Tauheed, Y.N. Joshi, E.H. Pinnington, J. Phys. B: At. Mol. Opt. Phys. **25**, L561 (1992)
6. M.O. Larsson, A.M. Gonzalez, R. Hallin, F. Heijkenskjöld, B. Nyström, G.O. Sullivan, C. Weber, A. Wånnström, Phys. Scripta **53**, 317 (1996)
7. M. Wang, M.O. Larsson, A. Arnesen, R. Hallin, F. Heijkenskjöld, C. Nordling, A. Wånnström, J. Opt. Soc. Am. B **13**, 2715 (1996)
8. M. Wang, M.O. Larsson, A. Arnesen, R. Hallin, F. Heijkenskjöld, C. Nordling, A. Wånnström, J. Opt. Soc. Am. B **14**, 1515 (1997)
9. M. Wang, A. Arnesen, R. Hallin, F. Heijkenskjöld, M.O. Larsson, A. Wånnström, A.G. Trigueiros, A.V. Loginov, J. Opt. Soc. Am. B **14**, 3277 (1997)
10. R. Sarmiento, J.G. Reyna Almandos, M. Raineri, M. Gallardo, J. Phys. B **32**, 2853 (1999)
11. J. Reyna Almandos, R. Sarmiento, M. Raineri, F. Bredice, M. Gallardo, J. Quant. Spectrosc. Radiat. Transf. **70**, 189 (2001)
12. É. Biémont, J.E. Hansen, C.J. Zeippen, *Astrophysical Applications of Powerful New Databases*, ASP Conference Series **78**, edited by S.J. Adelman, W.L. Wiese, (Astron. Soc. of Pacific, San Francisco, Calif., 1995), pp. 157-160
13. R.D. Cowan, *The Theory of Atomic Structure and Spectra* (Univ. of California Press, Berkeley, 1981)
14. P. Quinet, P. Palmeri, E. Biémont, M.M. McCurdy, G. Rieger, E.H. Pinnington, M.E. Wickliffe, J.E. Lawler, Mon. Not. R. Astron. Soc. **307**, 934 (1999)
15. J. Migdalek, W.E. Baylis, J. Phys. B: At. Mol. Phys. **11**, L497 (1978)
16. S. Fraga, J. Karwowski, K.M.S. Saxena, *Handbook of Atomic Data* (Elsevier, Amsterdam, 1976)
17. *Beam-foil spectroscopy*, edited by S. Bashkin (Springer-Verlag, 1976)
18. R. Hutton, Y. Zou, S. Huldt, I. Martinson, K. Ando, B. Nyström, T. Kambara, H. Oyama, Y. Awaya, Phys. Scripta T **80**, 552 (1999)
19. H.-P. Garnir, P.-H. Lefèbvre, Nucl. Instrum. Meth. B (in press, 2005)
20. F.S. Garnir-Monjoie, Y. Baudinet-Robinet, H.P. Garnir, P.D. Dumont, J. Phys. (France) **41**, 41 (1980)
21. L.J. Curtis, H.G. Berry, J. Bromander, Phys. Lett. A **34**, 169 (1971)
22. É. Biémont, P. Quinet, C. Zeippen, Phys. Scripta **71**, 163 (2005)
23. E.H. Pinnington, R.N. Gosselin, Q. Ji, J.A. Kernahan, B. Guo, Phys. Scripta **46**, 40 (1992)
24. W.R. Johnsson, Z.W. Liu, J. Sapirstein, At. Data Nucl. Data Tables **64**, 279 (1996)